Reprinted from *J. Mol. Biol.* (1983) **171**, 95–100

Divalent Cation Sites in Tomato Bushy Stunt Virus

Difference Maps at 2·9 Å Resolution

J. Hogle, T. Kirchhausen and S. C. Harrison

J. Mol. Biol. (1983) **171**, 95–100

LETTERS TO THE EDITOR

Divalent Cation Sites in Tomato Bushy Stunt Virus

Difference Maps at 2·9 Å Resolution

Difference electron density maps, using as few as four 1/2° oscillation photographs, have been computed for tomato bushy stunt virus crystals soaked in EDTA, $GdCl_3$ and silicotungstate. The maps define a double divalent cation site, responsible for regulating expansion of the virus particle, as well as sites for binding tungstate anions.

Properties of the tomato bushy stunt virus (TBSV) particle, for which a 2·9 Å resolution crystallographic structure determination has been described (Harrison *et al.*, 1978; Olson *et al.*, 1983), raise a number of questions concerning assembly and stability best answered by locating specific adducts. In particular, the role of divalent cations in a transition from the native form to an expanded structure prompts a search for cation binding sites, and indeed good candidates for such sites were noticed during initial inspection of the electron density map. The substantial effort required to collect and process data from crystals with such large unit cells has induced an effort to see how economically we can determine difference structures; that is, whether a relatively small fraction of a complete data set is sufficient, when coupled with excellent native phases and icosahedral averaging, to compute an interpretable difference map. We report here three such maps and their interpretation. The structures are: (1) virus treated with EDTA; (2) EDTA-treated virus with Gd^{3+} then added; (3) silicotungstate-treated virus. Good maps were calculated with data from as few as four 1/2° oscillation photographs. These structures have enabled us to locate sites we believe responsible for a Ca^{2+}-controlled structural transition.

Intensity data from the various derivatives were collected by oscillation photography and processed as described by Winkler *et al.* (1979). Only relatively sparse data sets were collected: about 30% of the reflections to 2·9 Å in the case of EDTA (7 acceptable photographs, 1/2° oscillation each), about 20% (4 photographs) for Gd^{3+}, and about 20% to 3·2 Å (4 photographs) for silicotungstate. Despite the meagre sampling, post-refinement calculations (Winkler *et al.*, 1979) were successful even with Gd^{3+} and silicotungstate data, using "safe" whole spots from the four films as a reference data base. Note that the high symmetry of the *I*23 space group ensures that on any single film there is uniform distribution of reflections throughout the asymmetric unit. Table 1 summarizes data collection statistics for the three forms. Derivative and native intensities were placed on a common scale by application of scale and "temperature" factors using a conventional Wilson plot-matching criterion, and amplitude differences greater than $(\sigma_N^2+\sigma_D^2)^{1/2}$ (where σ_N^2 and σ_D^2 represent scaled variances for native and derivative data: cf. Winkler *et al.*, 1979) were passed on to a Fast Fourier program (Ten Eyck, 1973). This standard deviation "filter" typically eliminated 50% to 60% of the differences, and the resulting maps thus

0022–2836/83/330095–06 $03.00/0

TABLE 1

Form	Reflections measured	Resolution range	Number of films ($\frac{1}{2}$° oscillation)	Reflections appearing on more than one film	R
EDTA	60,244	6·0 to 2·9 Å	7	9922	0·15
Gd^{+3}	39,039	6·0 to 2·9 Å	4	7147	0·23
STA	31,842	6·0 to 2·9 Å	4	1736	0·32
Native	182,000	6·0 to 2·9 Å			0·31

$R = \dfrac{\sum_h \sum_{j=1}^{N_h} |I_{h_j} - \bar{I}_h|}{\sum_h N_h \bar{I}_h}$, where the reflection, h, has been measured N_h times in data collection, and the average and differences are taken after appropriate scaling.

contained less than 10% of the total possible terms. Nonetheless, icosahedral averaging (Bricogne, 1976; Olson *et al.*, 1983) produced extremely clean difference maps, as can be judged from Figure 1.

The EDTA difference map, sections of which are shown in Figure 1(a), has only three sets of strong, icosahedrally distinct features. These are three pairs of density minima, quasi-equivalently related, all lying at subunit interfaces about 130 Å from the particle center. The two minima at each of the three positions are about 5 Å from each other, suggesting that two neighboring EDTA-chelatable ions are present. Positive contours are also present in these features; it is not clear at this time whether they represent side-chain motions that accompany chelation or whether they are largely Fourier "noise". The same two minima are also present in silicotungstate difference maps (Fig. 1(b)), of which the strong positive features will be discussed later. Silicotungstate at 10^{-4} M (pH 5) is apparently capable of abstracting divalent cations from these positions, analogous to EDTA.

One of the two deep minima in EDTA and silicotungstate maps corresponds to a site for UO_2^{2+} substitution in a derivative used for phasing (sites UA1, UB1 and UC1 described by Harrison *et al.*, 1978). The other coincides with a strong peak in the native maps already tentatively interpreted as a bound cation (Harrison *et al.*, 1978; Harrison, 1980). It is also the principal site of Gd^{+3} substitution, as seen in the difference map in Figure 1(c). We therefore refer to these as U and G sites, respectively. Three pairs of such sites, at S-domain interfaces as shown in Figure 2(a), constitute the only significant features in the EDTA difference map and the only important *negative* features in the silicotungstate difference map. As noted above, the refined native map shows a strong peak of density at the G site, but residual "heavy-atom artefacts" preclude clear interpretation of the U site in that map alone.

The chemistry of this double binding region is already relatively clear from the model (Olson *et al.*, 1983) and from chemical sequence data (P. Hopper, S. C. Harrison & R. Sauer, unpublished results). A sketch of the site appears in Figure 2(b). Five aspartic acid residues have been identified definitely, three from

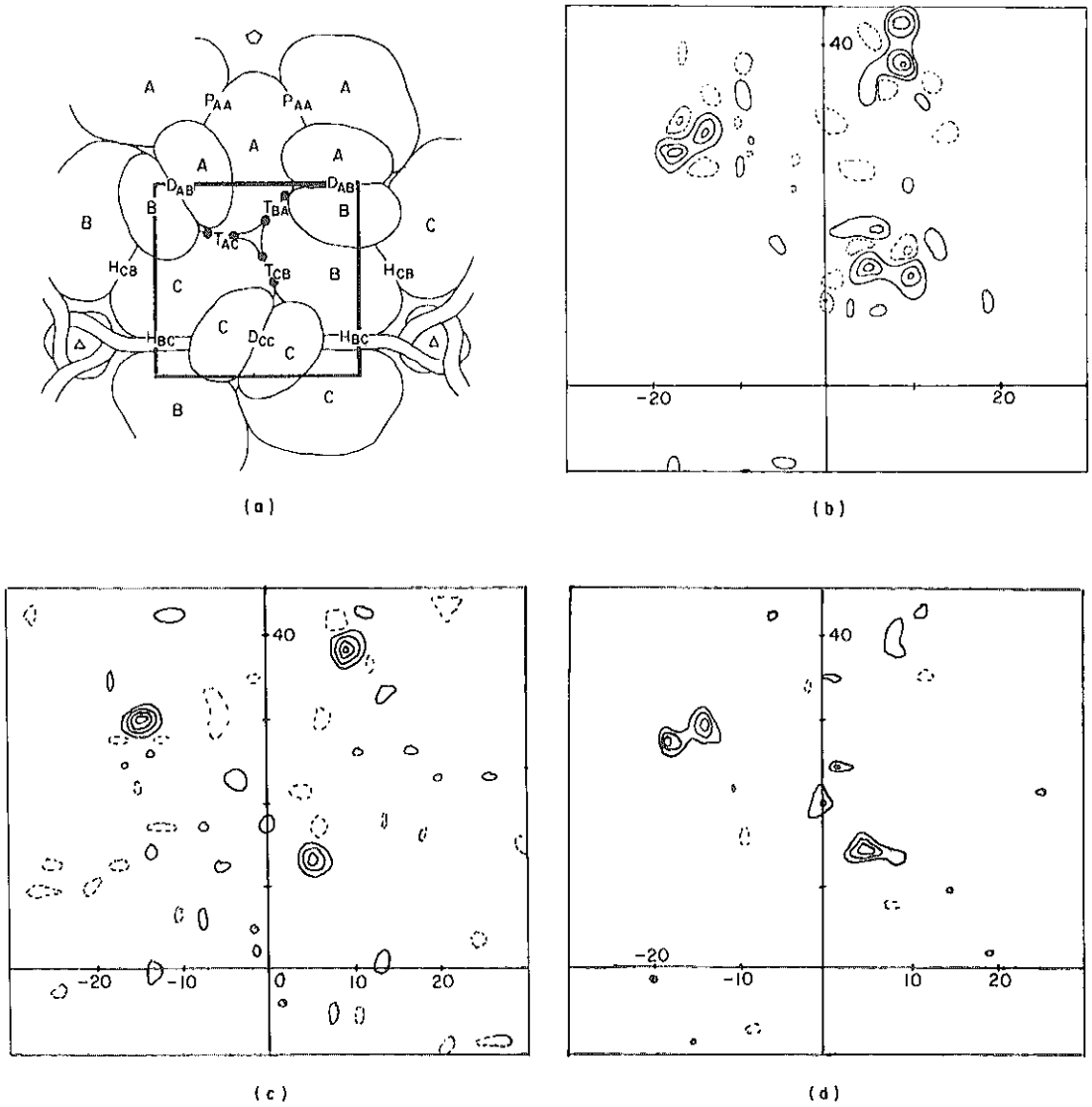

FIG. 1. Icosahedrally-averaged difference maps in divalent cation binding region. All maps are sections normal to z at $z = 130$ Å (see Olson *et al.*, 1983, for details of sectioning convention). (a) Location of map sections in the structure. (b) EDTA map. Solid contours are again "holes" in the EDTA-soaked crystal. The sites closer to the quasi-3-fold are the G sites, those farther from it, the U sites. (c) Silicotungstate map. Solid contours are again "holes", as in (a). This map is noisier than (a), but contains the same pairs of peaks. The A/B boundary sites are very weak, due either to incomplete abstraction of the cations or to inadequate data sampling. (d) Gd^{3+} map. Solid contours are positive density with respect to native.

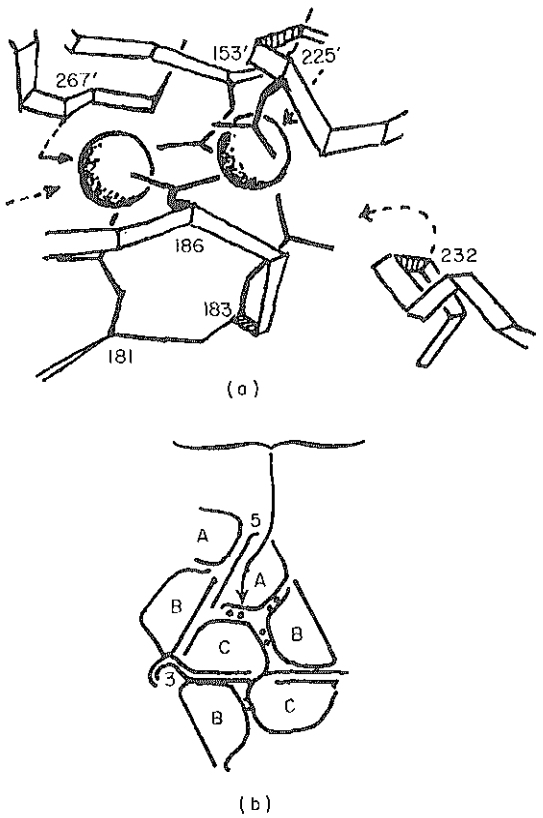

FIG. 2. (a) Divalent cation binding sites are indicated by dots in the packing diagram. (b) The C/A boundary site is shown in detail. Unprimed numbers refer to residues in C; primed numbers to A. Residues 153, 181, 183, 186 and 225 are aspartic acid; 232 is lysine; 267 is glutamine. Additional arrows are possible directions of ligation by water. The left-hand site is U; the right-hand site, G.

the subunit on one side of the interface, two from the other. Two of the aspartic acid residues (one from each subunit) appear shared between U and G; the other three (two from subunit C in the diagram in Fig. 2, one from A) appear confined to one or the other. We emphasize that this assignment is tentative, and refinement may alter our picture. It does give three negative charges to the G site and two to the U site, perhaps accounting for the selectivity of the former when a lanthanide ion is bound. A lysine residue may contribute to overall charge neutrality in the usual case.

We have not identified the ions chemically, but a number of arguments lead us to conclude that it is Ca^{2+}. The density appears too strong to be Mg^{2+} (it is significantly stronger than clearly identified H_2O sites, for example), and Mg^{2+} has no effect on particle expansion (S. C. Harrison, unpublished results). The ligands all appear to be carboxylate groups or water oxygen atoms (perhaps one carbonyl), as in known Ca^{2+} sites (Kretsinger & Nelson, 1976), rather than

nitrogen or sulphur atoms, as in protein Zn^{2+} sites. The substitution by Gd^{3+} and by UO_2^{2+} is also characteristic of Ca^{2+} positions.

TBSV has been shown to undergo a precise and reversible structural transition when divalent cations are chelated and pH raised above 7·0 (Robinson & Harrison, 1982; Krüse *et al.*, 1982). The high pH form is expanded by about 20 Å with respect to the native structure. Crystallographic analysis of expanded TBSV shows that the transition involves dissociation of just those interfaces at which the G and U sites are found (Robinson & Harrison, 1982). We therefore believe that these sites are the loci of control of expansion by divalent cations.

Silicotungstate has the structural formula $SiW_{12}O_{40}^{4-}$, but it tends to break down into smaller polytungstate anions in solution (Cotton & Wilkinson, 1962; Baker *et al.*, 1955). The W_{12} heteropolyacid is a cage-like structure, about 12 Å in diameter, with the 12 tungsten atoms at the vertices of a cubo-octahedron (Signer & Cross, 1934). The very strong intensity changes in the silicotungstate adduct are due mainly to occupancy of a site on the outer surface of the S domain of subunit C, in a corner formed partly by the lower edge of the P domain (Fig. 3). Sections through the difference map in this region show a shell of density, approximately 10 Å in diameter, corresponding clearly to some form of the heteropolyacid cage. Ligands include two basic residues (Lys276, Arg307) as well as other polar groups. The P-domain/S-domain relationship in the A/B conformation differs significantly

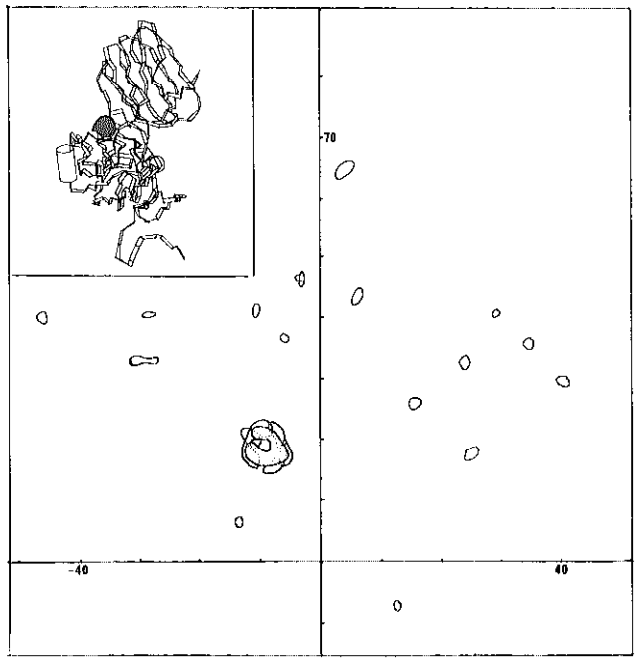

FIG. 3. Icosahedrally average silicotungstate difference map sectioned normal to z as in Fig. 1. Superimposed sections from $z = 137$ to 145 Å, showing single prominent feature centered at $x = -9$, $y = 18$. The inset drawing shows the position of the silicotungstate binding site on the subunit in the C conformation.

from that in C, accounting for the absence of silicotungstate sites on A and B subunits. The external silicotungstate cage is thus a C-conformation marker.

A set of less-pronounced peaks in the silicotungstate difference map decorates the inner surface of the S-domain. The most prominent correlate with positions on A and B-subunit arms, where diffuse features in the native electron density map indicate partly ordered sequences just N-terminal to the well-ordered S-domain. Others may be interpreted by assuming binding of some form of tungstate or polytungstate anion to inward-projecting arginine or lysine side-chains. The corresponding residues have been identified by chemical sequence (Hopper *et al.*, unpublished results), but side-chain density is often diffuse in the native map. These could represent RNA-phosphate binding positions, with considerable latitude in precise location of the phosphate ensured by side-chain flexibility.

We thank Craig Steele for assistance in all aspects of the computations. The work was supported by grants from NIH (CA-13202 to S.C.H.) and NSF (PCM-77-11398 to S.C.H., for computing hardware). J.H. acknowledges a postdoctoral fellowship from the American Cancer Society and S.C.H. acknowledges an Alfred Sloan Fellowship.

Harvard University
Department of Biochemistry and Molecular Biology
7 Divinity Avenue
Cambridge, MA 02138, U.S.A.

Received 26 April 1983

J. HOGLE†
T. KIRCHHAUSEN
S. C. HARRISON

REFERENCES

Baker, M. C., Lyons, P. A. & Singer, S. J. (1955). *J. Amer. Chem. Soc.* **77**, 2011–2012.
Bricogne, G. (1976). *Acta Crystallogr. sect. A*, **32**, 832–847.
Cotton, F. A. & Wilkinson, G. (1962). *Advanced Inorganic Chemistry*, Interscience, New York.
Harrison, S. C. (1980). *Biophys. J.* **32**, 139–151.
Harrison, S. C., Olson, A. J., Schutt, C. E., Winkler, F. K. & Bricogne, G. (1978). *Nature (London)*, **276**, 368–373.
Kretsinger, R. & Nelson, D. J. (1976). *Coord. Chem. Rev.* **18**, 29–124.
Krüse, J., Krüse, K. M., Witz, J., Chauvin, C., Jacrot, B. & Tardieu, A. (1982). *J. Mol. Biol.* **162**, 393–417.
Olson, A. J., Harrison, S. C. & Bricogne, G. (1983). *J. Mol. Biol.* **171**, 61–93.
Robinson, I. K. & Harrison, S. C. (1982). *Nature (London)*, **297**, 563–568.
Signer, R. & Cross, H. (1934). *Helv. Chim. Acta*, **17**, 1076.
Ten Eyck, L. (1973). *Acta Crystallogr. sect. A*, **29**, 183–191.
Winkler, F. K., Schutt, C. E. & Harrison, S. C. (1979). *Acta Crystallogr. sect. A*, **35**, 901–911.

Edited by A. Klug

† Present address: Scripps Clinic Research Foundation, 10666 North Torrey Pines Road, La Jolla, CA 92037, U.S.A.